The Astronomical Journal, 147:50 (12pp), 2014 March doi:10.1088/0004-6256/147/3/50

MAGNETIC ACTIVITY AND ORBITAL PERIOD VARIATION OF THE SHORT-PERIOD ECLIPSING BINARY DV Psc

Qing-feng Pi (皮青峰)[1,2], Li-Yun Zhang (张立云)[1,2,5], Zhong-mu Li (李忠木)[3], and Xi-liang Zhang (张西亮)[2,4]
[1] College of Science/Department of Physics & NAOC-GZU-Sponsored Center for Astronomy Research, Guizhou University, Guiyang 550025, China; liy_zhang@hotmail.com
[2] Key Laboratory for the Structure and Evolution of Celestial Objects, Chinese Academy of Sciences, Kunming 650011, China
[3] Institute for Astronomy and History of Science and Technology, Dali University, Dali 671003, China
[4] National Astronomical Observatories/Yunnan Observatory, Chinese Academy of Sciences, Kunming 650011, China
Received 2013 September 3; accepted 2013 November 26; published 2014 January 24

ABSTRACT

We present six new BVR_cI_c CCD light curves of a short-period RS CVn binary DV Psc obtained in 2010–2012. The light curve distortions change on both short and long timescales, which is explained by two starspots on the primary component. Moreover, five new flare events were detected and the flare ratio of DV Psc is about 0.082 flares per hour. There is a possible relation between the phases (longitude) of the flares and starspots for all of the available data of late-type binaries, which implies a correlation of the stellar activity of the spots and flares. The cyclic oscillation, with a period of 4.9 ± 0.4 yr, may result from the magnetic activity cycle, identified by the variability of Max. I–Max. II. Until now, there were no spectroscopic studies of chromospheric activity indicators of the H_β and H_γ lines for DV Psc. Our observations of these indicators show that DV Psc is active, with excess emissions. The updated $O - C$ diagram with an observing time span of about 15 yr shows an upward parabola, which indicates a secular increase in the orbital period of DV Psc. The orbital period secularly increases at a rate of $dP/dt = 2.0 \times 10^{-7}$ days yr^{-1}, which might be explained by the angular momentum exchanges or mass transfer from the secondary to primary component.

Key words: binaries: eclipsing – stars: chromospheres – stars: flare – stars: late-type – starspots

Online-only material: color figures, machine-readable and VO tables

1. INTRODUCTION

DV Psc (GSC0008-324, IRXS J001309+053550) is an RS CVn type eclipsing binary with a high-level surface activity, which is characterized by the light curve (LC) asymmetries (Robb et al. 1999; Zhang & Zhang 2007; Vaňko et al. 2007; Parimucha et al. 2010; Zhang et al. 2010), Ca II H and K emissions (Beers et al. 1994), and strong X-ray emission from the *ROSAT* survey (Bade et al. 1998). These findings reveal that DV Psc has a high level of magnetic activity.

The first LCs with remarkable asymmetry for DV Psc were obtained by Robb et al. (1999). Later, Lu et al. (2001) contributed a medium precision radial-velocity observation for the system and obtained a mass ratio of 0.702 ± 0.014. Salchi & Edalati (2003) explained the asymmetric light curve by a spot on the surface of the hotter component, and meanwhile yielded a detached near-contact configuration for the system. Zhang & Zhang (2007) obtained multi-color CCD *BVR* photometric observations and found that DV Psc is a detached, near-contact binary system with a mass ratio of 0.69 ± 0.005. Moreover, Parimucha et al. (2010) obtained preliminary orbital results using their photometric and spectroscopic observations. They also found considerable variation in the number, location, and diameter of the spots on both components. The first flare-like event was detected by Zhang et al. (2010), and they also revised the orbital parameters and obtained new starspot parameters in 2008. All published orbital parameters are listed in Table 1.

Robb et al. (1999) obtained a number of times of minimum light, and gave an ephemeris JD Hel.Min I = 2451451.7204(7)+0.30855(3)E for DV Psc. Later, Vaňko et al. (2007) revised the ephemeris. Zhang & Zhang (2007) revised the new ephemeris and first found that the $O-C$ diagram with a low range of observing times shows a weak downward parabola, indicating a secular decrease in the orbital period of DV Psc. Subsequently, new minimum times of DV Psc were published by several astronomers (Parimucha et al. 2009, 2011).

DV Psc is a very intriguing target for studying period variation and stellar magnetic activity (Robb et al. 1999; Zhang & Zhang 2007; Vaňko et al. 2007; Parimucha et al. 2010; Zhang et al. 2010; Pribulla et al. 2012). This is our second paper studying the magnetic activity of DV Psc, following the first paper (Zhang et al. 2010). In this paper, we present six new light curves taken in 2010–2012 and one spectra to analyze starspot evolution, flare events, and chromospheric emission.

2. OBSERVATIONS AND DATA REDUCTION

The CCD photometric observations of DV Psc were performed using the 85 cm telescope at Xinglong station of the National Astronomical Observatories of China (NAOC). The observational log is listed in Table 2. The photometer was equipped with a 1024 × 1024 pixel CCD and the standard Johnson–Cousins–Bessell set of BVR_cI_c filters (Zhou et al. 2009) were used. All observed CCD images were reduced by means of the IRAF package in the standard fashion (bias substraction, cosmic-ray removal, and flat-field correction using twilight sky exposure). Since the field of DV Psc is not crowded, the technique of aperture photometry was applied to extract the instrumental magnitudes. GSC0008-743 and GSC0008-949 served as comparison and check stars, respectively, and were also used in the first paper (Zhang et al. 2010). No light variability of the comparison and check stars was reported in the previous observations of these two stars by previous authors and we also observed no intrinsic variability. The magnitude differences of DV Psc and the comparison star (in the sense of DV Psc minus the comparison star) are displayed in Figure 1.

[5] Author to whom correspondence should be addressed.

Table 1
The Results of LC Analysis for DV Psc from 1999 to 2010

Element Parameters	1999 Robb et al. 1999	2007 Vaňko et al. 2007	2007 Zhang & Zhang 2007	2007 Zhang & Zhang 2007	2010 Parimucha et al. 2010	2010 Zhang et al. 2010
T_1(K)	4300	4350a	4450a	4450a		4450a
q	0.83	0.701 ± 2	0.693a	0.693a	0.690 ± 0.025a	0.693a
i (°)	71	81.85 ± 17	88.807 ± 0.249	88.807 ± 0.249	80.25 ± 0.11	74.267 ± 0.070
T_2(K)	3650	3725 ± 10	3618 ± 10	3614 ± 8		3712 ± 5
Ω_1		3.471 ± 9	3.7558 ± 0.0101	3.7777 ± 0.0045		3.610 ± 0.006
Ω_2		5.107 ± 5	3.9728 ± 0.0118	3.9776 ± 0.0068		3.836 ± 0.010
$L_1/(L_1+L_2)_B$		0.949 ± 2	0.926 ± 0.005			0.9180 ± 0.0018
$L_1/(L_1+L_2)_V$		0.936 ± 2	0.903 ± 0.003	0.902 ± 0.002		0.8886 ± 0.0019
$L_1/(L_1+L_2)_R$		0.923 ± 2	0.889 ± 0.003			0.8640 ± 0.0022
$L_1/(L_1+L_2)_I$						0.8154 ± 0.0023

Note. Parameters not adjusted in the solution are denoted by a mark a.

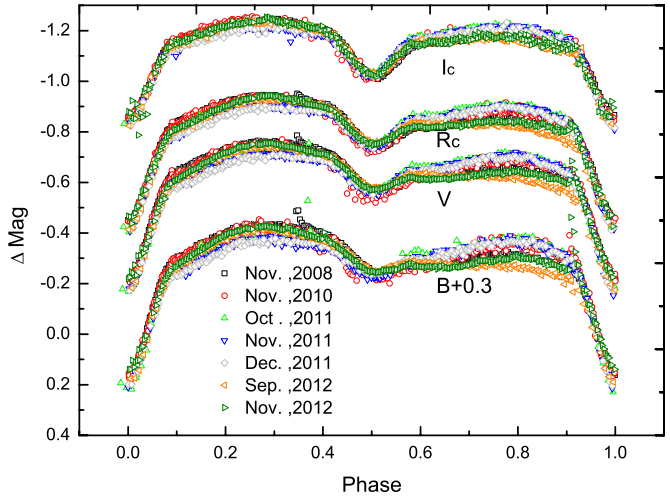

Figure 1. B, V, R_c, and I_c observations of DV Psc obtained at Xinglong station including published light curves by Zhang et al. (2010). Squares (□) indicate 2008 November 21 and 22 (Zhang et al. 2010), circles (○) – 2010 November 19, 20, and 21, triangles (△) – 2011 October 27, down triangles (▽) – 2011 November 12 and 13, diamonds (◇) – 2011 December 08 and 10, left triangles (◁) – 2012 September 04, and right triangles (▷) – 2012 November 16.

(A color version of this figure is available in the online journal.)

We neglected the second-order extinction effects because of the observational time and conditions. We did not perform photometric transformation with the international standard system. Different symbols represent data from the different seasons. The heliocentric Julian dates and magnitude differences between DV Psc and the comparison star are listed in Table 3. The errors of individual points do not exceed 0.01 mag in B, V, R_c, and I_c bands. For our observations, the phases of the data points were calculated using our new ephemeris defined later in Section 3.

One spectrum of DV Psc was obtained with the 2.16 m telescope at Xinglong station on 2012 February 15 (Figure 2). The OMR spectrograph centered at about 4280 Å with a reciprocal dispersion of 1.03 Å pixel^{-1} (Fang et al. 2010) and a 1340 × 240 pixel CCD were used. The spectral images were reduced using the IRAF package in the standard fashion. The wavelength calibration was made by taking the spectra of a He–Ar lamp. The observational exposure time was 15 minutes. The corresponding signal-to-noise ratio (S/N) is about 30.

Table 2
The Observational Log of DV Psc

Time	HJD (Start–End)	Phase (Start–End)	Band
2008 Nov 21	2454791.9225–2454792.1605	0.979–1.750	BVR_cI_c
2008 Nov 22	2454792.9175n–2454793.1611	0.204–0.994	BVR_cI_c
2010 Nov 19	2455519.9887–2455520.1570	0.709–1.255	BVR_cI_c
2010 Nov 20	2455520.9213–2455521.1600	0.732–1.506	BVR_cI_c
2010 Nov 21	2455521.9240–2455522.1885	0.982–0.839	BVR_cI_c
2011 Oct 27	2455861.9324–2455862.2603	0.007–1.048	BVR_cI_c
2011 Nov 12	2455877.9242–2455878.1915	0.817–1.684	BVR_cI_c
2011 Nov 13	2455878.9317–2455879.1974	0.083–0.944	BVR_cI_c
2011 Dec 8	2455903.9150–2455904.1220	0.056–0.727	BVR_cI_c
2011 Dec 10	2455905.9166–2455906.1430	0.543–0.277	BVR_cI_c
2012 Sep 4	2456175.0678–2456175.3798	0.903–1.909	BVR_cI_c
2012 Nov 16	2456247.9292–2456248.2330	0.052–1.037	BVR_cI_c

3. PERIOD STUDY

Based on our observations of DV Psc, new primary and secondary times of minimum light were obtained using the method of Kwee & van Woerden (1956) with polynomial fitting by the program of Nelson (2007). Because the asymmetric light curves affect the determination of the minima (Mikulášek et al. 2006; Pribulla et al. 2012), we only used observations around the primary and secondary minima in the phase intervals ±0.05 and ±0.04, respectively. This approach diminished the influence of the minimum asymmetries (van't Veer 1973). Moreover, these parts of the minima were found to be sufficiently symmetric. Table 4 lists the individual minimum light times and their weighted averages in the BVR_cI_c bands, together with their errors. In order to calculate an updated ephemeris and study the period variation, all published minimum times were collected from the literature and the Eclipsing Binaries Minima Database (available at http://var2.astro.cz/EN/; Paschke & Brat 2006). These data are listed in Table 5. The epochs of these minimum light times were calculated using a linear ephemeris (Zhang & Zhang 2007),

$$\begin{aligned}\text{Min.I} = {} & \text{JD(Hel.)}2454026.1424(\pm 0.0002) \\ & + 0.30853609^d(\pm 0.00000008)E, \end{aligned} \quad (1)$$

where E stands for epoch number. The revised linear ephemeride for DV Psc was determined to be

$$\begin{aligned}\text{Min.I} = {} & \text{JD(Hel.)}2454026.1429(\pm 0.0003) \\ & + 0.30853641^d(\pm 0.00000008)E. \end{aligned} \quad (2)$$

Table 3
BVR_c and I_c Photometric Data of DV Psc Taken in 2008, 2010, 2011, and 2012

B Band		*V* Band		R_c Band		I_c Band	
HJD	Δmag	HJD	Δmag	HJD	Δmag	HJD	Δmag
2454791.9225	−0.212	2454791.9228	−0.280	2454791.9229	−0.508	2454791.9231	−0.903
2454791.9234	−0.195	2454791.9236	−0.271	2454791.9238	−0.493	2454791.9240	−0.890
2454791.9242	−0.178	2454791.9245	−0.264	2454791.9247	−0.477	2454791.9249	−0.884
2454791.9251	−0.170	2454791.9254	−0.246	2454791.9256	−0.473	2454791.9257	−0.875
2454791.9260	−0.161	2454791.9263	−0.233	2454791.9265	−0.467	2454791.9266	−0.865
...	...	...	...	...	...	...	...
2456248.2285	−0.238	2456248.2304	−0.340	2456248.2306	−0.564	2456248.2307	−0.857
2456248.2290	−0.197	2456248.2314	−0.321	2456248.2316	−0.572	2456248.2317	−0.958
2456248.2300	−0.244	2456248.2324	−0.337	2456248.2326	−0.569	2456248.2328	−0.971
2456248.2310	−0.251	2456248.2334	−0.357	2456248.2336	−0.614	2456248.2338	−0.869
2456248.2320	−0.279	2456248.2344	−0.384	2456248.2346	−0.615	2456248.2348	−0.967
2456248.2330	−0.293	2456248.2354	−0.412	2456248.2357	−0.643	2456248.2358	−0.986

(This table is available in its entirety in machine-readable and Virtual Observatory (VO) forms in the online journal. A portion is shown here for guidance regarding its form and content.)

Table 4
Newly Obtained Times of Minimum Light of DV Psc

HJD (24,+) *B*	HJD (24,+) *V*	HJD (24,+) R_c	HJD (24,+) I_c	HJD (24,+) BVR_cI_c	Min.
54791.92940 ± 0.00010	54791.92950 ± 0.00010	54791.92940 ± 0.00010	54791.92950 ± 0.00010	54791.9295 ± 0.0001	Sec
55520.07855 ± 0.00151	55520.07868 ± 0.00087	55520.07826 ± 0.00075	55520.07823 ± 0.00054	55520.0784 ± 0.0009	Pri
55521.00431 ± 0.00055	55521.00419 ± 0.00036	55521.00367 ± 0.00029	55521.00364 ± 0.00023	55521.0040 ± 0.0004	Pri
55862.24548 ± 0.00042	55862.24566 ± 0.00030	55862.24525 ± 0.00046	55862.24523 ± 0.00016	55862.2454 ± 0.0003	Pri
55862.09181 ± 0.00020	55862.09267 ± 0.00023	55862.09179 ± 0.00013	55862.09140 ± 0.00133	55862.0919 ± 0.0005	Sec
55877.98086 ± 0.00142	55877.98060 ± 0.00009	55877.98024 ± 0.00093	55877.98043 ± 0.00088	55877.9805 ± 0.0009	Pri
55878.13762 ± 0.00026	±	55878.13603 ± 0.00007	55878.13472 ± 0.00006	55878.1361 ± 0.0001	Sec
55879.06210 ± 0.00073	55879.06165 ± 0.00026	55879.06072 ± 0.00034	55879.06013 ± 0.00029	55879.0612 ± 0.0004	Sec
55904.05443 ± 0.00100	55904.05424 ± 0.00100	55904.05251 ± 0.00171	55904.05147 ± 0.00138	55904.0532 ± 0.0013	Sec
55906.05775 ± 0.00044	55906.05747 ± 0.00037	55906.05743 ± 0.00091	55906.05717 ± 0.00066	55906.0575 ± 0.0006	Pri
56175.09801 ± 0.00005	56175.09807 ± 0.00029	56175.09800 ± 0.00032	56175.09732 ± 0.00020	56175.0979 ± 0.0002	Pri
56175.25612 ± 0.00028	56175.25612 ± 0.00028	56175.25520 ± 0.00006	56175.25397 ± 0.00005	56175.2554 ± 0.0001	Sec
56248.22220 ± 0.00143	56248.22167 ± 0.00156	56248.22124 ± 0.00163	56248.22204 ± 0.01570	56248.0710 ± 0.0000	Pri
56248.07340 ± 0.00004	56248.07095 ± 0.00001	56248.07075 ± 0.00003	56248.06886 ± 0.00004	56248.2218 ± 0.0015	Sec

Note. Pri—primary, Sec—Secondary.

The values of $(O-C)_1$ are listed in Column 5 of Table 5. The least-squares method with error−weight was applied in the calculating process. If there were no published errors, we had to use the average errors of our collected data. To clarify the period change, these values are shown in Figure 3, where an upward curve appears. The following quadratic ephemeris was obtained:

$$\begin{aligned}\text{Min.I} = {} & \text{JD(Hel.)}2454026.1420(\pm 0.0019) \\ & + 0.30853635^d(\pm 0.00000005)E \\ & + 8.4(\pm 1.0) \times 10^{-11}E^2. \end{aligned} \quad (3)$$

This ephemeris indicates a secular increase in the orbital period of DV Psc. The quadratic ephemeris resulted in a smaller sum of squares of the residuals (0.0006) than the result (0.001) of the linear least squares fit. With the coefficient of the quadratic term, we obtained a continuous period increase rate $dP/dt = 2.0 \pm 0.2 \times 10^{-7}$ days yr^{-1}.

4. ANALYSIS OF DV Psc

We will analyze the photometric starspot activity and chromospheric emission of DV Psc in this section.

4.1. Photometric Starspot Analysis

A comparison of LCs from 2008, 2010, 2011, and 2012 indicates both short-term and long-term variations. The new multi-color LCs were analyzed using the 2003 version of the W-D program (Wilson & Devinney 1971; Wilson 1990, 1994; Wilson & Van Hamme 2004). Individual points in the BVR_cI_c bands (excluding the flares) were used directly for photometric analysis, and the four light curves were simultaneously solved. We fixed some orbital parameters with the temperature of the primary component (4450 K) and the mass ratio (0.69) published in previous studies (Lu et al. 2001; Zhang & Zhang 2007; Parimucha et al. 2010). The temperature of the secondary (3712 K), the orbital inclination (74.°2), the dimensionless potentials of the two components, and the monochromatic luminosity of the primary were taken from our previous paper (Zhang et al. 2010). The telescope and comparison star used for the light curves in 2008 are the same for the new data. We fixed the orbital parameters (including the secondary temperature) and only adjusted the starspot parameters, because we thought the light curve distortions were only affected by starspots. Similar methods were used to discuss the starspot of RT And (Pribulla et al. 2000; Zhang & Gu 2007) and XY Uma (Pribulla

Table 5
The Minimum Times of DV Psc

JD(Hel.)24,+	Error	Method	Cycle	$(O-C)_1$	$(O-C)_2$	(Reference)
51408.8340	0.0003*	ccd	−8483.0	.0054	−.0003	(1)
51451.8770	0.0003*	ccd	−8343.5	.0076	.0021	(2)
51453.8792	0.0003*	ccd	−8337.0	.0043	−.0012	(2)
51454.8043	0.0003*	ccd	−8334.0	.0038	−.0017	(2)
51454.9620	0.0003*	ccd	−8333.5	.0072	.0017	(2)
51455.7301	0.0003*	ccd	−8331.0	.0040	−.0014	(2)
51455.8871	0.0003*	ccd	−8330.5	.0067	.0013	(2)
51460.8232	0.0003*	ccd	−8314.5	.0063	.0009	(2)
51460.9757	0.0003*	ccd	−8314.0	.0045	−.0009	(2)
51461.7499	0.0003*	ccd	−8311.5	.0073	.0019	(2)
51461.9009	0.0003*	ccd	−8311.0	.0041	−.0013	(2)
51474.7081	0.0003*	ccd	−8269.5	.0070	.0016	(2)
52920.0394	0.0001	ccd	−3585.0	−.0004	−.0008	(3)
52920.1955	0.0003	ccd	−3584.5	.0014	.0010	(3)
52920.9653	0.0005	ccd	−3582.0	−.0002	−.0006	(3)
52921.2735	0.0001	ccd	−3581.0	−.0005	−.0009	(3)
53258.8140	0.0002	ccd	−2487.0	.0012	.0014	(4)
53258.9677	0.0003	ccd	−2486.5	.0006	.0008	(4)
53284.4221	0.0001	ccd	−2404.0	.0007	.0009	(5)
53285.3479	0.0001	ccd	−2401.0	.0009	.0011	(5)
53285.5025	0.0002	ccd	−2400.5	.0013	.0015	(5)
53344.2782	0.0001	ccd	−2210.0	.0007	.0010	(5)
53618.5659	0.0001	ccd	−1321.0	−.0004	.0002	(6)
53637.3862	0.0001	ccd	−1260.0	−.0008	−.0001	(6)
53640.4720	0.0001	ccd	−1250.0	−.0004	.0003	(6)
53648.3397	0.0002	ccd	−1224.5	−.0004	.0003	(6)
53648.4938	0.0001	ccd	−1224.0	−.0005	.0002	(6)
53666.3867	0.0002	ccd	−1166.0	−.0027	−.0020	(7)
53667.4640	0.0001	ccd	−1162.5	−.0053	−.0046	(7)
53668.3987	0.0001	ccd	−1159.5	.0038	.0045	(7)
53668.7040	0.0003	ccd	−1158.5	.0005	.0012	(8)
53671.3290	0.0001	ccd	−1150.0	.0029	.0036	(6)
53963.5049	0.0001	ccd	−203.0	−.0051	−.0042	(6)
53965.5111	0.0004	ccd	−196.5	−.0044	−.0035	(6)
53972.4523	0.0001	ccd	−174.0	−.0053	−.0044	(6)
53974.4580	0.0001	ccd	−167.5	−.0051	−.0042	(6)
53995.4397	0.0001	ccd	−99.5	−.0038	−.0029	(6)
54006.2415	0.0003*	ccd	−64.5	−.0008	.0001	(9)
54007.1667	0.0003*	ccd	−61.5	−.0012	−.0003	(9)
54007.3215	0.0003*	ccd	−61.0	−.0007	.0002	(9)
54021.0503	0.0003*	ccd	−16.5	−.0018	−.0009	(9)
54025.0615	0.0003*	ccd	−3.5	−.0015	−.0006	(9)
54025.2180	0.0003*	ccd	−3.0	.0007	.0016	(9)
54025.9873	0.0003*	ccd	−.5	−.0013	−.0004	(9)
54026.1431	0.0003*	ccd	.0	.0002	.0011	(9)
54026.2961	0.0001	ccd	.5	−.0011	−.0002	(6)
54026.4530	0.0001	ccd	1.0	.0016	.0025	(6)
54027.3771	0.0001	ccd	4.0	.0001	.0010	(6)
54027.9944	0.0003*	ccd	6.0	.0003	.0012	(9)
54028.1482	0.0003*	ccd	6.5	−.0002	.0007	(9)
54035.3992	0.0001	ccd	30.0	.0002	.0011	(6)
54088.9299	0.0003*	ccd	203.5	−.0002	.0007	(10)
54110.9900	0.0003*	ccd	275.0	−.0005	.0004	(10)
54404.4076	0.0004	ccd	1226.0	−.0009	−.0001	(7)
54410.2698	0.0002	ccd	1245.0	−.0009	−.0001	(7)
54410.4260	0.0002	ccd	1245.5	.0010	.0018	(7)
54433.2610	0.0002	ccd	1319.5	.0043	.0051	(7)
54715.4127	0.0001	ccd	2234.0	−.0006	.0000	(7)
54715.5771	0.0002	ccd	2234.5	.0095	.0101	(7)
54716.4977	0.0002	ccd	2237.5	.0045	.0051	(7)
54737.3162	0.0002	ccd	2305.0	−.0032	−.0026	(7)
54737.4691	0.0003	ccd	2305.5	−.0045	−.0039	(7)
54739.3226	0.0002	ccd	2311.5	−.0022	−.0016	(7)
54748.4252	0.0002	ccd	2341.0	−.0015	−.0010	(7)
54751.0515	0.0003*	ccd	2349.5	.0023	.0028	(11)
54751.1998	0.0003*	ccd	2350.0	−.0037	−.0032	(11)
54755.9897	0.0003*	ccd	2365.5	.0039	.0044	(12)
54761.0758	0.0003*	ccd	2382.0	−.0008	−.0003	(12)
54791.9295	0.0001	ccd	2482.0	−.0008	−.0003	(15)
55060.5125	0.0003	ccd	3352.5	.0012	.0013	(14)
55064.5248	0.0002	ccd	3365.5	.0026	.0027	(14)
55090.4418	0.0002	ccd	3449.5	.0025	.0026	(14)
55097.3813	0.0002	ccd	3472.0	−.0001	.0000	(14)
55501.2574	0.0002	ccd	4781.0	.0019	.0011	(14)
55504.0348	0.0003*	ccd	4790.0	.0025	.0017	(11)
55504.1939	0.0003*	ccd	4790.5	.0073	.0065	(11)
55506.9643	0.0003*	ccd	4799.5	.0009	.0001	(12)
55520.0784	0.0009	ccd	4842.0	.0022	.0014	(15)
55521.0040	0.0004	ccd	4845.0	.0022	.0014	(15)
55861.0111	0.0003*	ccd	5947.0	.0021	.0003	(12)
55862.0919	0.0005	ccd	5950.5	.0030	.0012	(15)
55862.2454	0.0003	ccd	5951.0	.0023	.0005	(15)
55877.9805	0.0009	ccd	6002.0	.0020	.0002	(15)
55878.1361	0.0001	ccd	6002.5	.0034	.0016	(15)
55878.9046	0.0003*	ccd	6005.0	.0005	−.0013	(12)
55879.0612	0.0004	ccd	6005.5	.0029	.0011	(15)
55886.0029	0.0003*	ccd	6028.0	.0025	.0006	(11)
55904.0532	0.0013	ccd	6086.5	.0034	.0015	(15)
55906.0575	0.0006	ccd	6093.0	.0022	.0003	(15)
56175.0979	0.0002	ccd	6965.0	−.0012	−.0040	(15)
56175.2554	0.0001	ccd	6965.5	.0021	−.0007	(15)
56248.0710	0.0000	ccd	7201.5	.0031	.0000	(15)
56248.2218	0.0015	ccd	7202.0	−.0004	−.0035	(15)
56155.2004	0.0003*	ccd	6900.5	.0019	−.0008	(11)
56158.2872	0.0003*	ccd	6910.5	.0034	.0006	(11)
56160.1374	0.0003*	ccd	6916.5	.0024	−.0004	(11)
56160.2880	0.0003*	ccd	6917.0	−.0012	−.0040	(11)
56219.9911	0.0003*	ccd	7110.5	.0000	−.0030	(16)
56221.9956	0.0003*	ccd	7117.0	−.0010	−.0040	(16)

Notes. The data from $O-C$ gateway by mark (*), http://var.astro.cz/ocgate/.
References. (1) Paschke A*; (2) Robb et al. 1999; (3) Kim et al. 2006; (4) Krajci 2006; (5) Pribulla et al. 2005; (6) Parimucha et al. 2007; (7) Parimucha et al. 2009; (8) Dvorak 2006; (9) Zhang & Zhang 2007; (10) Nakajima K*; (11) Itoh H*; (12) Nagai K*; (13) Diethelm R*; (14) Parimucha et al. 2011; (15) This study; (16) Kiyota Seiichiro.

et al. 2001). We only adjusted the spot parameters and performed the spot fittings, using a model with two spots on the primary because the case of two spots being on the primary component is the most successful for explaining the distortion of the light curves (Zhang et al. 2010). Since a spot area is highly correlated with starspot temperature and latitude, the latitudes of both spots were assumed to be 90°, which means that their centers are on the equator of the component. Therefore, three adjustable parameters are the longitude, temperature, and radius of the spot. The details of the procedure for adjusting the starspot parameters are similar to the previous analysis methods of RT And (Zhang & Gu 2007) and DV Psc (Zhang et al. 2010). After many runs, we adjusted the spot parameters separately until the theoretical curves fit the observed ones well; the convergent solutions for the spots are given in Table 6. The errors of our obtained parameters come from the covariance matrix of the least-squares fit, and thus are only formal errors. The theoretical and observed LCs are plotted in Figure 4. The three-dimensional models of Roche geometry are shown in Figure 5.

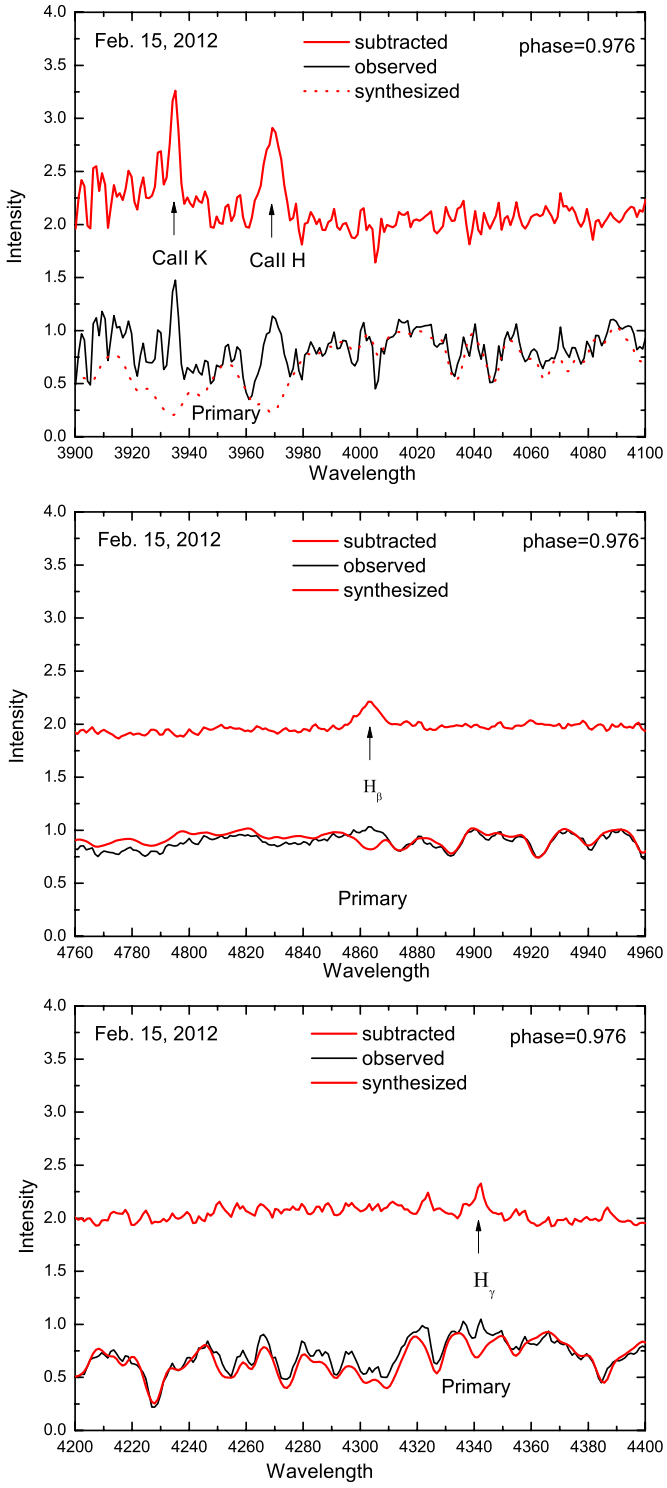

Figure 2. Observed, synthesized, and subtracted spectra containing the Ca II H and K, H_β, and H_γ lines. The dotted lines represent the synthesized spectra and the upper are the subtracted ones.

(A color version of this figure is available in the online journal.)

4.2. Chromospheric Activity Analysis

The Ca II H and K, H_β, and H_γ lines are very useful active diagnostic indicators in the middle chromosphere for late-type stars (Montes et al. 1995, 2004; Zhang & Gu 2008; Zhang 2011). Our normalized spectra of DV Psc were analyzed using the spectral subtraction technique with the program STARMOD

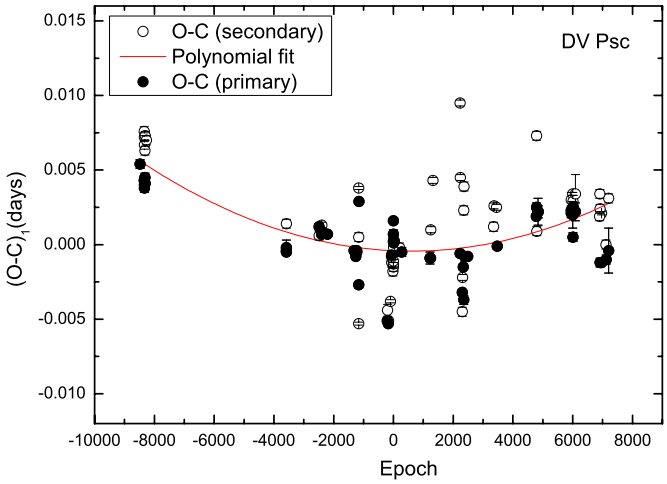

Figure 3. Period analysis of DV Psc.

(A color version of this figure is available in the online journal.)

(Barden 1985; Montes et al. 1995). For DV Psc, The intensity weight (0.89/0.11), which was used in the spectral subtraction procedure, was obtained from photometric light curve modeling. This method was also used to discuss the chromospheric activity of the eclipsing binary ER Vul by Gunn & Doyle (1997). HR1614 (K4V) and HR2458 (M1V) were used as templates for DV Psc. The synthesized and subtracted spectra containing Ca II H and K, H_β, and H_γ lines are displayed in Figure 2, where the upper solid lines represent the subtracted spectra and the lower solid and dotted lines indicate the observed and synthesized spectra, respectively.

5. DISCUSSION AND CONCLUSIONS

In this section, we discuss the period variation, starspot and flare events, and chromospheric emission.

5.1. The Period Variation

The orbital period of DV Psc may be increasing at the rate of $dP/dt = 2.0\times10^{-7}$ days yr^{-1}, as mentioned above. The period variation can be explained by mass transfer or magnetic braking (Applegate 1992; Lanza et al. 1998; Hoffman et al. 2006;). Since DV Psc is a detached, near-contact binary system (Zhang & Zhang 2007; Zhang et al. 2010; Parimucha et al. 2010), the period variation might be caused by mass transfer from the secondary (less massive) component to the primary component. On the other hand, the period decrease might be due to magnetic braking (Applegate 1992; Lanza et al. 1998). However, Zhang & Zhang (2007) found that the $O-C$ diagram shows a downward parabola, indicating a secular decrease. Considering our longer time span compared to that of Zhang & Zhang (2007), our new results are more likely to be reliable. It is too early to decide the character of the period variation using the $(O-C)$ diagram, based on the short time span of 15 yr. Therefore, new observations over the next 15–20 yr are required.

5.2. Starspot Evolution and Magnetic Cycle

The remarkable asymmetries of the light curves of DV Psc suggest the presence of high-level surface activities, which are explained by the two starspots on the primary. The most reliable spot parameter determined by the traditional light curve method is the active-region longitude (Berdyugina 2005). For the starspot parameters of DV Psc from the data set taken in

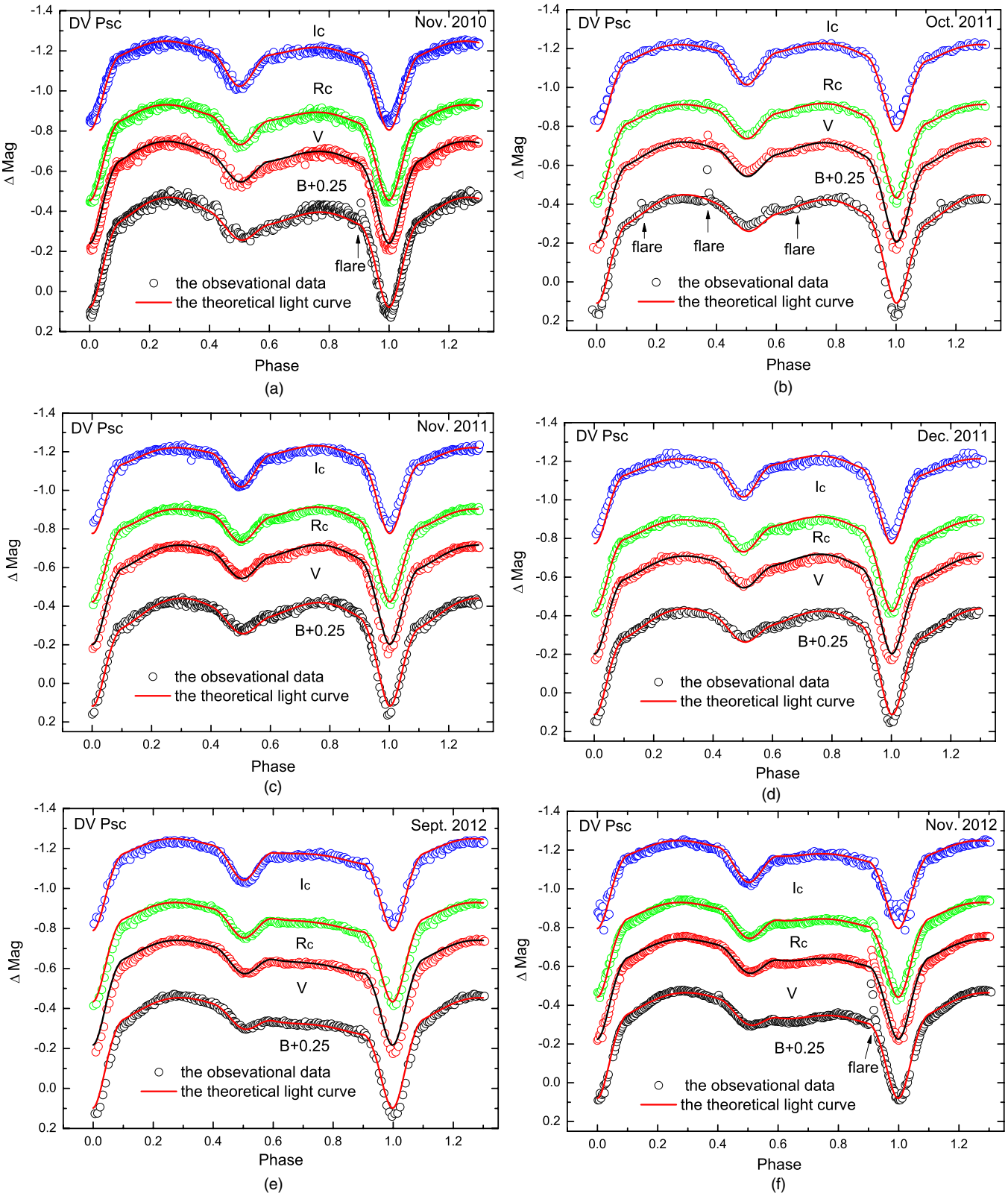

Figure 4. Observational and theoretical light curves of DV Psc. The points represent the observational data and the solid lines represent the theoretical light curves. (A color version of this figure is available in the online journal.)

2008, the longitudes of two active regions are 130°.8 and 266°.5, respectively (Zhang et al. 2010). However, the longitudes of spot1 and spot2 were 119° and 264°.1, respectively, in 2010 November. It indicates that the longitude of spot1 changed over a long timescale (about two years). The three observations in 2011 showed that spot1 was at longitudes of 48°.7, 55°.3, and 55°.0, respectively. Two observations in 2012 reveal that spot1 is concentrated at longitudes of 145°.5 and 144°.8, while spot2 is at

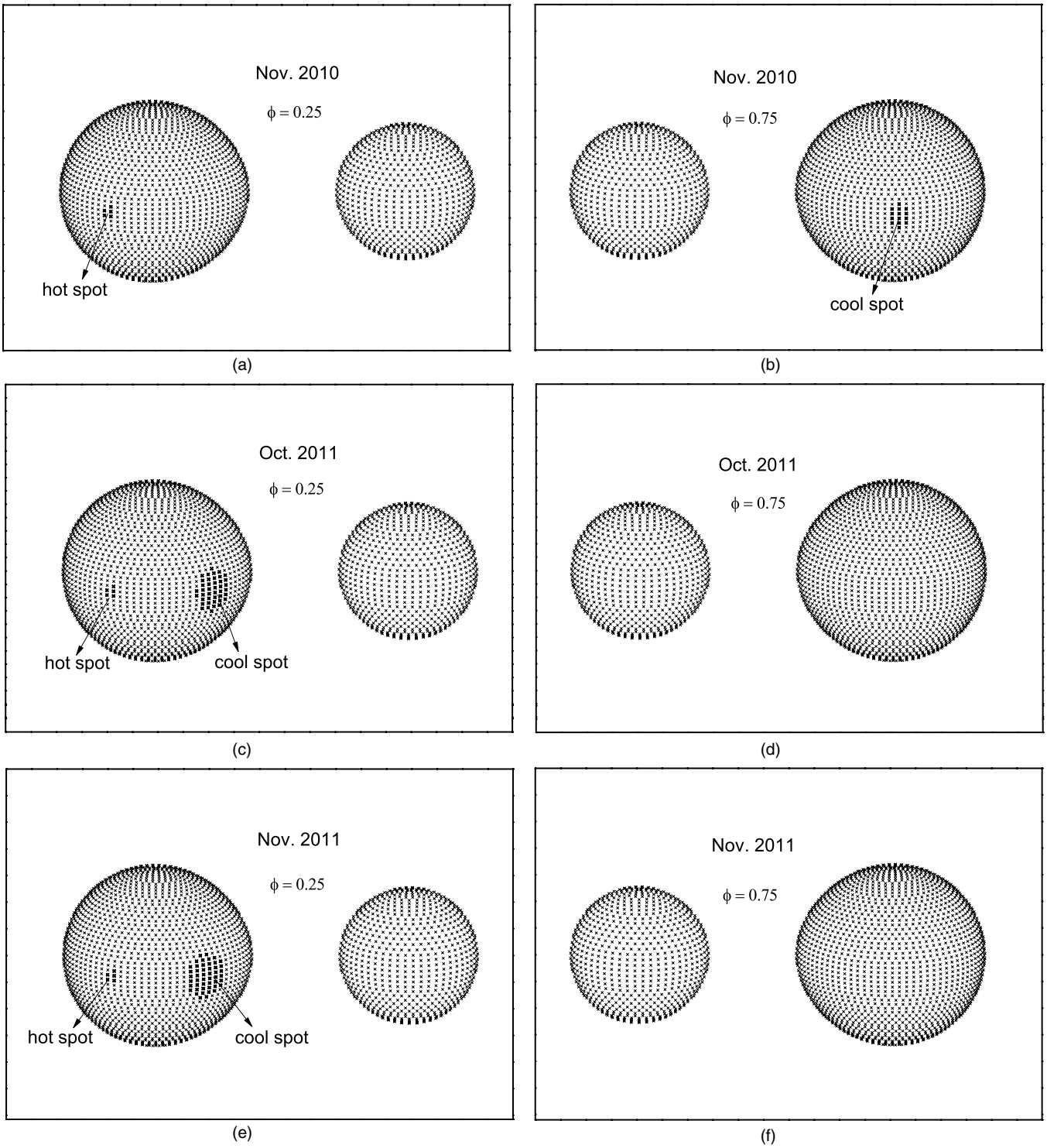

Figure 5. Configuration and spot distribution of DV Psc in phases 0.25 and 0.75 in different seasons.

longitudes of 286.°4 and 270.°6, respectively. From Table 6 and Figure 5, one can see that starspots evolve not only on a short timescale (about two months) but also on a long timescale (one year). Our new results confirm that DV Psc has considerable variations in starspot parameters (Robb et al. 1999; Zhang & Zhang 2007; Vaňko et al. 2007; Parimucha et al. 2010; Zhang et al. 2010).

From the LCs taken in 1999 (Robb et al. 1999), in 2007 (Zhang & Zhang 2007), in 2008 (Parimucha et al. 2010; Zhang et al. 2010), and in 2012 (this paper), one can see that Max. I (phase 0.25) is brighter than Max. II (phase 0.75). However, Max. I became fainter than Max. II in 2006 (Parimucha et al. 2010) and in 2007 October (Zhang & Zhang 2007). The values of the light curves of Max. I and Max. II were used by many astronomers to search the magnetic cycle (Pribulla et al. 2001; Yang et al. 2012). To examine the variation outside the eclipse of DV Psc, we collected the values of Max. I–Max. II from the previously published observations (Robb et al. 1999; Zhang &

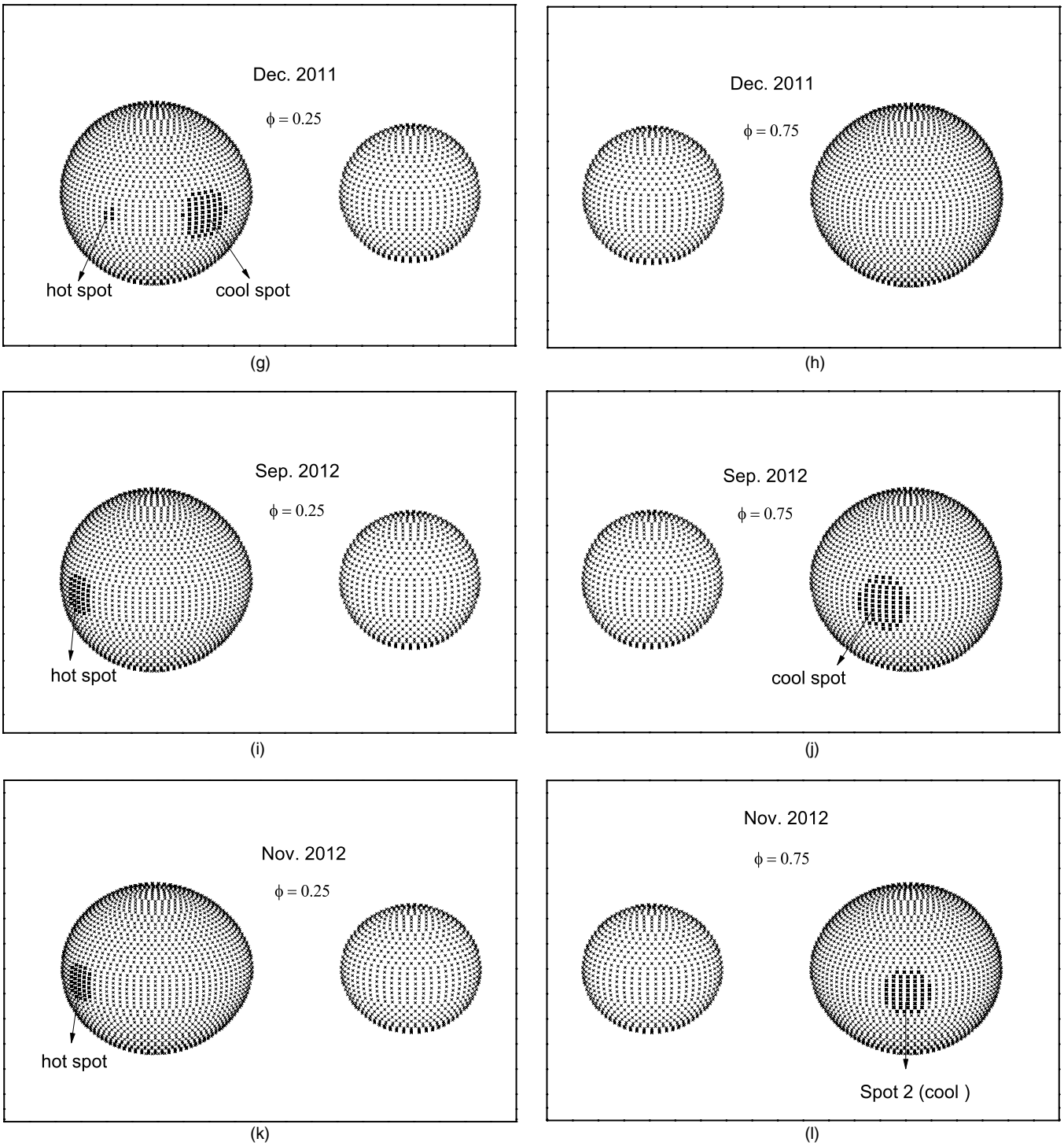

Figure 5. (Continued)

Zhang 2007; Parimucha et al. 2010; Zhang et al. 2010), which are listed in Table 7. In order to search the activity cycle, a sinusoidal function analysis was performed using the least-squares method; a similar function was also used by Pribulla et al. (2000) to search the magnetic cycle of RT And. The results are displayed in Figure 6. The resulting magnetic cycles of the different bands are 4.89 ± 0.38 yr in the *B* band, 4.88 ± 0.33 yr in the *V* band, 4.86 ± 0.27 yr in the R_c band, and 5.0 ± 0.60 yr in the I_c band. The average magnetic cycle of DV Psc is 4.88 ± 0.32 yr.

5.3. Flare

Flares are known as sudden and violent events that release magnetic energy. For DV Psc, the first flare event was detected in phase 0.35 on 2008 November 22 (Zhang et al. 2010). During our observations, five new flare-like events were detected (one flare event in phase 0.90 on 2010 November 20, three flares in phases 0.15, 0.37, and 0.67 on 2011 October 27, and one flare in phase 0.91 on 2012 November 16). The criteria to identify a flare are as follows: a flare should last for several minutes

Table 6
The Spot Parameters of DV Psc

Year	Spot1					Spot2					Reference
	P/S	Colatitude	Longitude	Radius	T (s)	P/S	Colatitude	Longitude	Radius	T (s)	
1997	S	0°	270°	20°	...	...	...	...	...	...	1
2005	P	90°	202° ± 25°	8° ± 3°	4785 K	S	90°	190° ± 25°	10° ± 3°	4098 K ± 10 K	2
2006 Sep	S	117.°8 ± 1.°3	65.°9 ± 0.°9	31.°3 ± 0.°6	2403 K ± 134 K	S	94.°9 ± 1.°5	125.°4 ± 1.°1	5.°9 ± 0.°7	6898 K ± 223 K	3
2006 Oct	S	113.°8 ± 0.°6	67.°4 ± 0.°5	32.°9 ± 0.°4	2314 K ± 89 K	...	...	...	...	...	3
2008 Dec	P	90°a	266.°5 ± 0.°1	12.°9 ± 0.°1	2181 K ± 301 K	P	90°a	130.°8 ± 0.°1	5.°6 ± 0.°2	6087 K ± 53 K	4
2010 Nov	P	90°a	264.°1 ± 0.°1	8.°2 ± 0.°1	2181 K ± 301 K	P	90°a	119.°0 ± 0.°1	4.°7 ± 0.°1	6087 K ± 53 K	5
2011 Oct	P	90°a	48.°7 ± 0.°5	13.°9 ± 0.°1	3847 K ± 26 K	P	90°a	119.°0 ± 0.°1	4.°7 ± 0.°1	6087 K ± 53 K	5
2011 Nov	P	90°a	55.°3 ± 0.°5	14.°5 ± 0.°3	3847 K ± 26 K	P	90°a	119.°0 ± 0.°1	4.°7 ± 0.°1	6087 K ± 53 K	5
2011 Dec	P	90°a	55.°0 ± 0.°3	16.°4 ± 0.°3	3847 K ± 26 K	P	90°a	119.°0 ± 0.°1	4.°7 ± 0.°1	6087 K ± 53 K	5
2012 Sep	P	90°a	286.°4 ± 0.°2	17.°2 ± 0.°1	3451 K ± 35 K	P	90°a	145.°5 ± 0.°2	13.°4 ± 0.°2	4936 K ± 20 K	5
2012 Nov	P	90°a	270.°6 ± 0.°1	16.°2 ± 0.°1	3476 K ± 33 K	P	90°a	144.°8 ± 0.°3	13.°4 ± 0.°1	4965 K ± 22 K	5

Notes. Parameters not adjusted in the solution are denoted by mark (a). P-Primary, S-Secondary.
References. (1) Robb et al. 1999; (2) Vaňko et al. 2007; (3) Zhang & Zhang 2007; (4) Zhang et al. 2010; (5) This study.

Table 7
The Magnitude Difference of DV Psc in Phases 0.25 and 0.75 in Different Observing Seasons

Year	B (mag)	V (mag)	R_c (mag)	I_c (mag)	Reference
1997	...	...	−0.097*	...	(1)
2005	0.041*	0.037*	0.017*	0.018*	(2)
2006	0.064*	0.053*	0.032*	0.018*	(2)
2006 Sep	0.011*	0.014*	0.012*	...	(3)
2006 Oct	...	0.019*	...	...	(3)
2008	−0.105*	−0.093*	−0.089*	−0.046*	(2)
2008 Dec	−0.114	−0.101	−0.082	−0.049	(4)
2010 Nov	−0.052	−0.052	−0.042	−0.030	(5)
2011 Oct	0.012	0.009	0.002	0.004	(5)
2011 Nov	0.002	0.003	0.002	0.003	(5)
2011 Dec	0.004	0.004	0.005	0.014	(5)
2012 Nov	−0.134	−0.114	−0.097	−0.057	(5)
2012 Dec	−0.130	−0.111	−0.090	−0.061	(5)

Notes. The estimated data from literature by mark (*).
References. (1) Robb et al. 1999; (2) Parimucha et al. 2010; (3) Zhang & Zhang 2007; (4) Zhang et al. 2010; (5) This study.

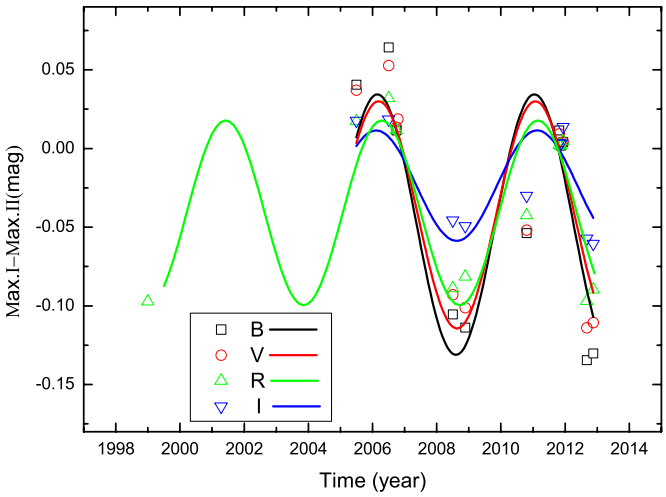

(a) B band

Figure 6. Magnitude differences (Max. I−Max. II) of BVR_cI_c bands vs. observing time of DV Psc. Different symbols represent different bands, and the solid lines represent the corresponding sin fit.
(A color version of this figure is available in the online journal.)

and contain more than two data points (not due to cosmic rays from the direction of the stars), and the amplitude of the peak should be greater than 0.03 mag (three times the photometric error of about 0.01 mag) in the B and V bands. These criteria were also used in Qian et al. (2012). The flares are shown in Figure 7 (B and V bands) and the parameters are listed in Table 7. The observations in the B and V bands demonstrate that DV Psc exhibits flare activity. We also found two flares in similar phases (phase 0.9 and phase 0.37). In total, DV Psc was monitored photometrically for 73.5 hr (Table 2), which revealed a flare rate of about 0.082 flares per hour. We have also photometrically collected flares of late-type binaries, as listed in the Table 8, where the star name, observing band, phases of the flare and starspot, flare rise time (s), flare decay time (s), flare total duration (s,) and flare amplitude (mag) are listed. The relation between the flare amplitude and duration time of late-type binaries is shown in Figure 8, where the solid lines present linear fits to individual band data. As shown in Figure 8, it seems that flare amplitudes of late-type stars increase with the increases in their durations, and the trends are basically consistent with each other in the $UBVR_c$ bands (excluding the I band; the data of the flare in the I_c band are too few and their amplitudes are very small in the I_c band). More data are needed to confirm this. We also checked the relation between the phases of the flares and the spot positions for all available data (see Table 8). The phases of the flare and starspot are plotted in Figure 9. With the least-squares method, the linear relation was obtained as

$$\text{Flare phase} = 0.06(\pm 0.11) + 0.99(\pm 0.21)\ \text{spot phase}. \quad (4)$$

The slope of the relation is about 1, which indicates that the phases of the flares were close to the positions of the starspots. This implies a correlation of the stellar activity of spots and flares.

5.4. Chromospheric Activity

From our newly observed spectra of DV Psc, we can see that the chromospheric activity indicators, the H_β and H_γ lines, show strong filled-in absorption (Figure 2). Application

Table 8
The Properties of the Flares and Starspots on Late-type Binaries

Stare Name	Flare Phase	Spot Phase	Filter	Rise Time (minute)	Decay Time (minute)	Total Duration (minute)	Amplitude (mag)	Reference
SV Cam			*U*	16	27	43	0.12 ± 0.01	(1)
SV Cam			*B*	16	27	43	0.05 ± 0.01	(1)
SV Cam			*V*	16	27	43	0.03 ± 0.01	(1)
SV Cam			*U*	11	7	18	0.15 ± 0.01	(1)
SV Cam			*B*	4	7	11	0.06 ± 0.01	(1)
SV Cam			*V*	3	7	10	0.03 ± 0.01	(1)
SV Cam			*U*	6	13	9	0.05 ± 0.01	(1)
SV Cam			*B*	4	6	10	0.03 ± 0.01	(1)
XY Uma			*U*	...	...	30	0.33	(2)
XY Uma			*B*	...	...	30	0.13	(2)
XY Uma			*V*	...	...	30	0.09	(2)
V711 Tau			*U*	138.6	45	285	0.61	(3)
V711 Tau			*B*	144	43.8	247.8	0.27	(3)
V711 Tau			*V*	133	43.8	262.8	0.18	(3)
II Peg			*B*	3.52	7.00	10.52	0.066 ± 0.01	(4)
II Peg			*U*	23.00	78.00	101.00	0.371 ± 0.02	(4)
II Peg			*U*	1.80	9.08	10.88	0.207 ± 0.03	(4)
II Peg			*U*	...	...	4.9	0.08	(5)
II Peg			*U*	...	...	11.2	0.13	(5)
II Peg			*U*	...	...	4.0	0.13	(5)
II Peg			*U*	...	...	7.8	0.11	(5)
II Peg			*U*	...	...	14.1	0.08	(5)
WY Cnc	0.1	0.1	*B*	...	...	64	0.134	(6)
WY Cnc	0.1	0.1	*V*	...	...	64	0.062	(6)
WY Cnc	0.1	0.1	*R*	...	...	64	0.045	(6)
FR Cnc			*B*	...	...	41	1.02	(7)
FR Cnc			*V*	...	...	41	0.49	(7)
FR Cnc			*R*	...	...	41	0.21	(7)
FR Cnc			*I*	...	...	41	0.14	(7)
CM Dra			*I*	...	...	60	0.05	(8)
CM Dra			*U*	...	...	75	0.7	(9)
CM Dra			*I*	...	...	60	0.05	(9)
CM Dra			*B*	...	...	108	0.20	(9)
CM Dra			*R*	...	...	92	0.21	(10)
CM Dra			*R*	...	...	70	0.10??	(10)
CM Dra			*R*	...	...	21	0.03??	(10)
CM Dra			*R*	...	...	34	0.21	(10)
CM Dra			*R*	...	...	60	0.23	(11)
CM Dra			*R*	...	...	135	0.04	(11)
CM Dra			*R*	...	...	135	0.08	(11)
CM Dra			*R*	...	...	135	0.09	(11)
CM Dra			*R*	...	...	34.2	0.02	(11)
CM Dra			*R*	...	...	40.2	0.02	(11)
V405 And	0.8		*B*	...	...	223.2	0.60	(12)
V405 And	0.8		*V*	...	...	109	0.27	(12)
V405 And	0.8		*R*	...	...	80	0.12	(12)
V405 And	0.8		*I*	...	...	91	0.08	(12)
DK Cvn	0.50	0.4	*B*	9.5	71.9	81.4	0.668	(13)
DK Cvn	0.0	0.81	*B*	6.1	24.6	30.7	0.516	(14)
DK Cvn	0.44	0.52	*B*	10.4	15.7	26.1	0.901	(14)
DK Cvn	0.47	0.52	*B*	5.2	10.4	15.7	0.488	(14)
DK Cvn	0.0	0.81	*V*	6.1	24.6	30.7	0.244	(14)
DK Cvn	0.43	0.52	*V*	5.2	10.5	15.7	0.180	(14)
DK Cvn	0.0	0.81	*R*	6.1	24.6	30.7	0.220	(14)
CU Cnc			*R*	...	...	73	0.52	(15)
CU Cnc			*R*	...	...	17	0.10	(15)
CU Cnc			*R*	...	...	23	0.05	(15)
CU Cnc			*R*	...	...	38	0.04	(15)
DV Psc	0.35	0.36	*B*	3.4	10.1	13.5	0.067	(16)
DV Psc	0.35	0.36	*V*	3.4	10.1	13.5	0.040	(16)
DV Psc	0.35	0.36	R_c	3.4	10.1	13.5	0.020	(16)
DV Psc	0.91	0.73	*B*	1.8	7.5	9.3	0.091	(17) 20/11/2010
DV Psc	0.15	0.14	*B*	3.2	3.25	6.45	0.043	(17) 27/10/2011
DV Psc	0.37	0.33	*B*	5.0	7.48	12.48	0.161	(17) 27/10/2011
DV Psc	0.37	0.33	*V*	2.48	5.00	7.48	0.051	(17) 27/10/2011

Table 8
(Continued)

Stare Name	Flare Phase	Spot Phase	Filter	Rise Time (minute)	Decay Time (minute)	Total Duration (minute)	Amplitude (mag)	Reference
DV Psc	0.67	0.33	*B*	3.3	6.62	9.92	0.037	(17) 27/10/2011
DV Psc	0.91	0.75	*B*	1.45	8.25	9.30	0.206	(17) 16/11/2012
DV Psc	0.91	0.75	*V*	2.51	6.78	9.30	0.089	(17) 16/11/2012
NSVS07453183	0.40	0.72	*V*	32	84	116	0.1	(18)
NSVS07453183			*R*	32	84	116	0.076	(18)
NSVS07453183			*I*	32	84	116	0.05	(18)
CG Cyg	0.33	0.2	*R*				0.01	(19)

References. (1) Patkós 1981; (2) Zeilik et al. 1982; (3) Zhang et al. 1990; (4) Doyle et al. 1993; (5) Byrne et al. 1995; (6) Kozhevnikova et al. 2006; (7) Golovin et al. 2007; (8) Lacy 1977; (9) Kim et al. 1997; (10) Kozhevnikova et al. 2004; (11) Nelson & Caton 2007; (12) Vida et al. 2009; (13) Terrell et al. 2005; (14) Dal et al. 2012; (15) Qian et al. 2012; (16) Zhang et al. 2010; (17) This study; (18) Zhang et al. 2012; (19) Heckert & Zeilik 1989.

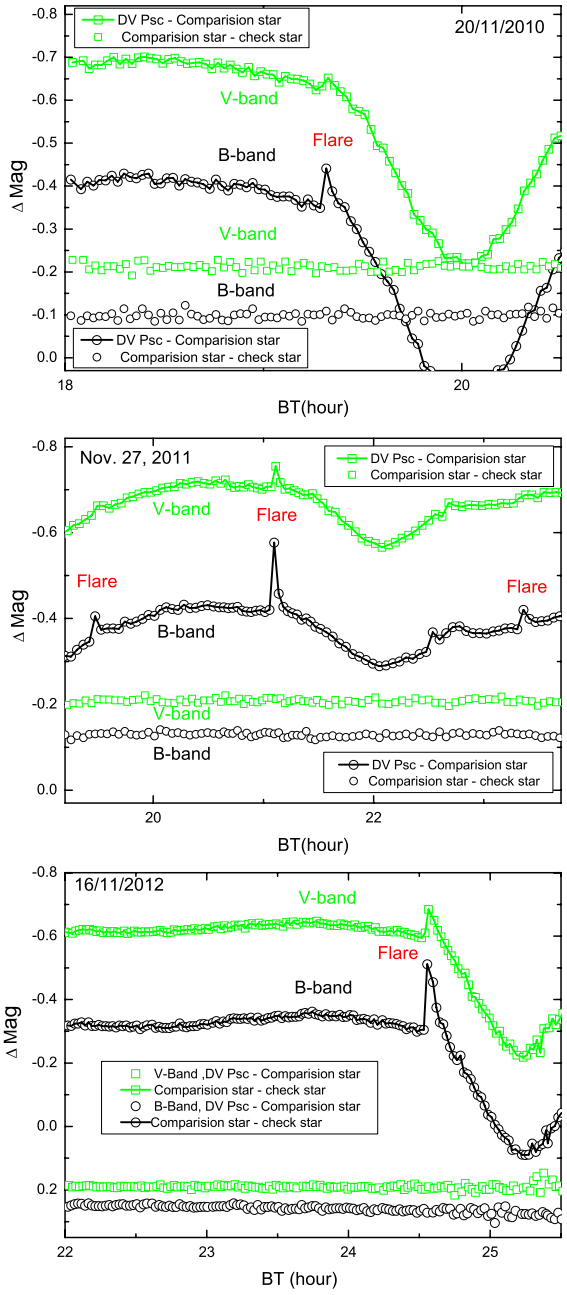

Figure 7. Flares of DV Psc in the *B* and *V* bands on 2010 November 20, 2011 October 27, and 2012 November 16, as well as the magnitude differences between the check and comparison stars.

(A color version of this figure is available in the online journal.)

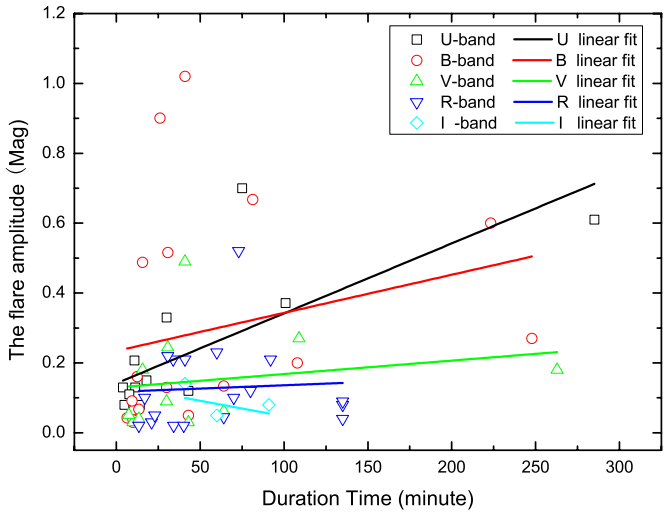

Figure 8. Relation of the flare amplitude vs. duration time of late-type stars in $UBVR_cI_c$ bands. Different colors represent the different bands, and the solid lines represent the linear fits.

(A color version of this figure is available in the online journal.)

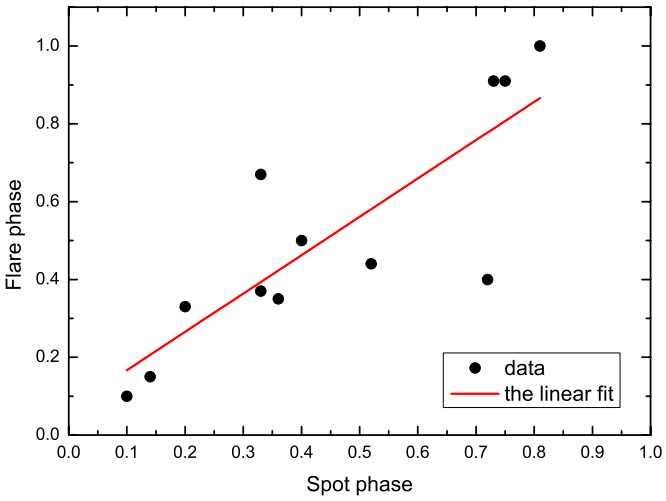

Figure 9. Relation of the phase of the flare vs. the spot phase of late-type binaries. The solid line represents the linear fit.

(A color version of this figure is available in the online journal.)

of the spectral subtraction technique reveals that these lines exhibit weak excess emissions. The Ca II H and K lines show strong filled-in absorption with self-reversal core emission, and the corresponding subtraction spectra exhibit obvious excess

emission, which are consistent with the result derived by Beers et al. (1994). All of these indicate that the chromosphere of DV Psc is active, which might be due to the presence of the plage-like regions. For DV Psc, the chromospheric emission is consistent with the starspot and flare event in the photosphere. These results indicate that DV Psc has very strong magnetic activity.

The authors are very grateful to Han J. L., Zhou A. Y., Yang Y. G., and Fang X. S. and the observing assistants at the 85 cm telescope of the Xinglong station for their kind help during our observations. The authors are also grateful for the help from the Research Group for Compact Objects and Diffuse Medium, NAOC. This work is supported by the NSFC under grant Nos. 10978010, 11263001, U1231102, 11203005, and 11203070. This work was partially supported by the Open Project Program of the Key Laboratory of Optical Astronomy, NAOC, and The Key Laboratory for the Structure and Evolution of Celestial Objects, Chinese Academy of Sciences.

REFERENCES

Applegate, J. H. 1992, ApJ, 385, 621
Bade, N., Engels, D., Voges, W., et al. 1998, A&AS, 127, 145
Barden, S. C. 1985, ApJ, 295, 162
Beers, T. C., Bestman, W., & Wilhelm, R. 1994, AJ, 108, 268
Berdyugina, S. V. 2005, LRSP, 2, 8
Byrne, P. B., Panagi, P. M., & Lanzafame, A. C. 1995, A&A, 299, 115
Dal, H. A., Sipahi, E., & Özdarcan, O. 2012, PASA, 29, 150
Doyle, J. G., Mathioudakis, M., & Murphy, H. M. 1993, A&A, 278, 499
Dvorak, S. W. 2006, IBVS, 5677, 1
Fang, X. S., Gu, S. H., Cheung, S. L., et al. 2010, RAA, 10, 253
Golovin, A., Pavlenko, E., Kuznyetsova, Y., & Krushevska, V. 2007, IBVS, 5748, 1
Gunn, A. G., & Doyle, J. G. 1997, A&A, 318, 60
Heckert, P. A., & Zeilik, M. 1989, IBVS, 3294
Hoffman, D. I., Harrison, T. E., McNamara, B. J., et al. 2006, AJ, 132, 2260
Kim, S. L., Chun, M. Y., Lee, W. B., & Doyle, L. 1997, IBVS, 4462, 1
Kim, C.-H., Lee, C.-U., Yoon, Y.-N., et al. 2006, IBVS, 5694, 1
Kozhevnikova, A. V., Alekseev, I. Yu., Heckert, P. A., & Kozhevnikov, V. P. 2006, IBVS, 5723, 1
Kozhevnikova, A. V., Kozhevnikov, V. P., Zakharova, P. E., et al. 2004, in IAU Symp. 223, Multi-Wavelength Investigations of Solar Activity, ed. A. V. Stepanov, E. E. Benevolenskaya, & A. G. Kosovichev (Cambridge: Cambridge Univ. Press), 687
Krajci, T. 2006, IBVS, 5690, 1
Kwee, K. K., & van Woerden, H. 1956, BAN, 12, 327
Lacy, C. H. 1977, ApJL, 218, L444
Lanza, A. F., Rodonò, M., & Rosnor, R. 1998, MNRAS, 296, 893
Lu, W. X., Rucinski, S. M., & Ogloza, W. 2001, AJ, 122, 402
Mikulášek, Z., Wolf, M., Zejda, M., et al. 2006, Ap&SS, 304, 363
Montes, D., Crespo-chaón, i., Gálvez, M. C., et al. 2004, LNEA, 1, 119
Montes, D., Fernández-Figueroa, M. J., De Castro, E., & Cornide, M. 1995, A&A, 294, 165
Nelson, R. H. 2007, Software by Bob Nelson, http://members.shaw.co/bob.nelson/software1.htm
Nelson, T. E., & Caton, D. B. 2007, IBVS, 5789, 1
Parimucha, Š., Dubovsky, P., Baludansky, D., et al. 2009, IBVS, 5898, 1
Parimucha, Š., Dubovsky, P., Vanko, M., et al. 2011, IBVS, 5980, 1
Parimucha, Š., Pribulla, T., Rucinski, S., et al. 2010, in ASP Conf. Ser. 435, Binaries—Key to Comprehension of the Universe, ed. A. Prša & M. Zejda (San Francisco, CA: ASP), 99
Parimucha, Š., Vanko, M., Pribulla, T., et al. 2007, IBVS, 5777, 1
Paschke, A., & Brat, L. 2006, OEJV, 23, 13
Patkós, L. 1981, ApL, 22, 131
Pribulla, T., Baludansky, D., Chochol, D., et al. 2005, IBVS, 5668, 1
Pribulla, T., Chochol, D., Heckert, P. A., et al. 2001, A&A, 371, 997
Pribulla, T., Chochol, D., Milano, L., et al. 2000, A&A, 362, 169
Pribulla, T., Vaňko, M., Ammler-von Eiff, M., et al. 2012, AN, 333, 754
Qian, S. B., Zhang, J., Zhu, L. Y., et al. 2012, MNRAS, 423, 3646
Robb, R. M., Wagg, J., Berndsen, A., Desroches, L., et al. 1999, IBVS, 4800
Salchi, F., & Edalati, M. T. 2003, Ap&SS, 288, 217
Terrell, D., Koff, R. A., & Henden, A. A. 2005, IBVS, 5642, 1
Vaňko, M., Parimucha, Š., & Pribulla, T. 2007, AN, 328, 655
van't Veer, F. 1973, A&A, 26, 357
Vida, K., Oláh, K., Kovári, Zs., et al. 2009, A&A, 504, 1021
Wilson, R. E., & Devinney, E. J. 1971, ApJ, 166, 605
Wilson, R. E. 1990, ApJ, 356, 613
Wilson, R. E. 1994, PASP, 106, 921
Wilson, R. E., & Van Hamme, W. 2004, Computing Binary Star Observables, privately circulated monograph, 1
Yang, Y. G., Qian, S. B., & Soonthornthum, B. 2012, AJ, 143, 122
Zeilik, M., Elston, R., & Henson, G. 1982, IBVS, 2200, 1
Zhang, X. B., & Zhang, R. X. 2007, MNRAS, 382, 1133
Zhang, L. Y., & Gu, S. H. 2007, A&A, 471, 219
Zhang, L. Y., & Gu, S. H. 2008, A&A, 487, 709
Zhang, L. Y., Zhang, X. L., & Zhu, Z. Z. 2010, NewA, 16, 362
Zhang, L. Y. 2011, in ASP Conf. Ser. 451, 9th Pacific Rim Conference on Stellar Astrophysics, ed. S. Qain, K. Leung, L. Zhu, & S. Kwok (San Francisco, CA: ASP), 123
Zhang, L. Y., Li, Z. M., Pi, Q. F., et al. 2012, arXiv:1209.1574
Zhang, R.-X., Zhai, D.-S., & Zhang, X.-B. 1990, IBVS, 3456, 1
Zhou, A. Y., Jiang, X. J., Zhang, Y. P., et al. 2009, RAA, 9, 349